Faraday Discussions

Accepted Manuscript

This manuscript will be presented and discussed at a forthcoming Faraday Discussion meeting. All delegates can contribute to the discussion which will be included in the final volume.

Register now to attend! Full details of all upcoming meetings: http://rsc.li/fd-upcoming-meetings

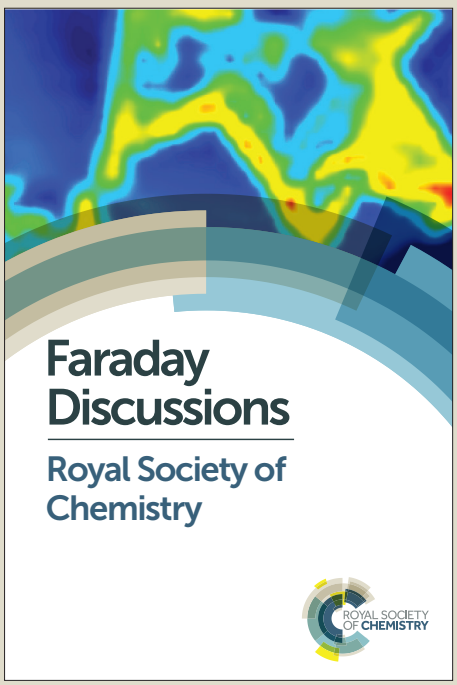

This is an *Accepted Manuscript*, which has been through the Royal Society of Chemistry peer review process and has been accepted for publication.

Accepted Manuscripts are published online shortly after acceptance, before technical editing, formatting and proof reading. Using this free service, authors can make their results available to the community, in citable form, before we publish the edited article. We will replace this *Accepted Manuscript* with the edited and formatted *Advance Article* as soon as it is available.

You can find more information about *Accepted Manuscripts* in the Information for Authors.

Please note that technical editing may introduce minor changes to the text and/or graphics, which may alter content. The journal's standard Terms & Conditions and the Ethical guidelines still apply. In no event shall the Royal Society of Chemistry be held responsible for any errors or omissions in this *Accepted Manuscript* or any consequences arising from the use of any information it contains.

ROYAL SOCIETY OF CHEMISTRY

www.rsc.org/faraday_d

Co-electrolysis of steam and CO_2 in full-ceramic symmetrical SOECs: A strategy for avoiding the use of Hydrogen as a safe gas.

M.Torrell[1], S. García-Rodríguez[2], A. Morata[1], G. Penelas[2], A. Tarancón[1]

[1] Catalonia Institute for Energy Research (IREC), Jardins de les Dones de Negre, 1, 08930-Sant Adrià de Besòs, Barcelona, Spain; *

atarancon@irec.cat

[2] REPSOL Technology Center, Ctra de Extremadura A-5, km 18, 28935 Móstoles, Madrid, Spain.

Abstract

The use of cermets as fuel electrodes for solid oxide electrolysis cells requires permanent circulation of reducing gas, e.g. H_2 or CO, so called safe gas, in order to avoid oxidation of the metallic phase. Replacing metallic based electrodes by pure oxides is therefore proposed as an advantage for the industrial application of solid oxide electrolyzers. In this work, full-ceramic symmetrical solid oxide electrolysis cells have been investigated for steam/CO_2 co-electrolysis. Electrolyte supported cells with $La_{0.75}Sr_{0.25}Cr_{0.5}Mn_{0.5}O_{3-\delta}$ reversible electrodes have been fabricated and tested in co-electrolysis mode using different fuel compositions, from pure H_2O to pure CO_2, at temperatures of 850°C – 900°C.

Electrochemical impedance spectroscopy and galvanostatic measurements have been carried out for the mechanistic understanding of the symmetrical cells performance. The content of H_2 and CO in the product gas has been measured by in-line gas micro-chromatography. The effect of employing H_2 as a safe gas has been also investigated. Maximum density currents of 750 mA/cm^2 and 620 mA/cm^2 have been applied at 1.7 V for pure H_2O and for H_2O:CO_2 ratios of 1:1, respectively. Remarkable results were obtained for hydrogen-free fuel compositions, which confirmed the interest of using ceramic oxides as a fuel electrode candidate to reduce or completely avoid the use of safe gas in

Faraday Discussions Accepted Manuscript

operation minimizing the contribution of the reverse water shift reaction (RWSR) in the process. H_2:CO ratios close to two were obtained for hydrogen-free tests fulfilling the basic requirements for synthetic fuel production. An important increase of the operation voltage was detected under continuous operation leading to a dramatic failure by delaminating of the oxygen electrode.

Faraday Discussions Accepted Manuscript

Introduction

Massive emissions of anthropogenic carbon dioxide are destabilizing the natural carbon cycle. New strategies for the conversion and valorization of CO_2 are today considered with much attention since they can reduce the climate change impact while giving new opportunities for sustainable industrial development [1]. One of the main routes for CO_2 valorization is based on its chemical transformation for the generation of high-added value products. In particular, employing CO_2 as a carbon source allows the generation of hydrocarbon fuels by following Power-to-Fuel (P2F) schemes. Power to fuel is a set of technologies that allow the conversion of electricity into a fuel. The conversion of electricity surplus into easy-to-transport and –storage fuels might play a crucial role in future energy strategies based on large-scale energy storage and the interconnection of the two major energy infrastructures currently available, i.e. fuel and electricity networks.

High temperature electrolysis (HTE) is one of the most promising alternatives for the generation of gas fuel from electricity due to its high efficiency and flexibility [2]. In particular, solid oxide electrolysis cells (SOECs) seem to be a strong candidate because of their low internal resistances that allow high production rates at low voltages [2]. Moreover, besides typical steam electrolysis for direct hydrogen production, high temperature SOECs can efficiently electrolyze other molecules like CO_2 that, as previously mentioned, could be employed as the main carbon source for producing C-based chemicals. By introducing CO_2 and H_2O as a fuel, SOECs are able to generate CO and H_2, i.e. syngas. The fabrication of syngas is considered the first step for the production of synthetic hydrocarbons since it is the precursor of high added value hydrocarbons through well-known Fischer-Tröpsch catalytic routes [3]. When the electricity employed in the electrolysis comes from free carbon and renewable energy sources, this synthetic fuel production scheme becomes a sustainable route.

Faraday Discussions Accepted Manuscript

Favorable thermodynamic conditions permit the reduction of the electrical consumption in SOECs (compared to low T electrolysis). Part of the energy needed for the electrolysis reactions is provided in the form of heat, which can eventually come from waste heat in other industrial processes increasing the overall efficiency. The main advantage of simultaneous electrolysis of CO_2 and H_2O is the low polarization resistance (with values similar to the pure steam electrolysis) and the negligible reduction of CO to carbon [4,6]. This coke deposition takes place following the Boudouard reaction that is favored at low temperatures and high concentrations of CO, i.e. opposite to high temperature and low CO concentrations typically found in solid oxide electrolysis. After first evidences of co-electrolysis reported by A.O. Isenberg [5], one of the first major descriptions of co-electrolysis using SOECs were published by Stoots et al. in 2008 [6] and have been followed by an increase on the research activity during the last years [3, 6-17]. However, the co-electrolysis in SOECs is still under study since it is a more complicated process than pure steam or carbon dioxide electrolysis, involving different reactions competing in the typical operation conditions. The current understanding of the co-electrolysis is not complete yet since the controlling mechanism depends on the kinetics of the multiple reactions, i.e. it is dependent on the catalysts involved. In this sense, it has not been shown yet if the syngas generation by co-electrolysis of steam and CO_2 actually proceeds by simultaneous electrolysis of both CO_2 and H_2O or by predominant steam electrolysis combined to reverse water shift reaction (RWSR) (hydrogen production by electrolysis that immediately reacts with CO_2 to produce CO) [18].

Since CO and CO_2 are similarly present in Solid Oxide Fuel Cells (SOFCs), even being carbon monoxide a typical fuel, the same materials employed in SOFCs and SOECs have been used for the first prototypes of co-electrolysers of solid oxide cells (SOCs) [10]. However, standard Ni-based fuel electrodes can cause problems in electrolysis because the poor redox stability and the possible carbon deposition at high CO_2 concentrations,

Faraday Discussions Accepted Manuscript

especially in dry CO_2 [9, 19]. To avoid dramatic effects due to redox cycles, SOECs based on Ni-cermets usually employ hydrogen as a safe gas during operation. However, simple recirculation of hydrogen in co-electrolysis systems is unpractical and, therefore, it is of great interest to find more redox stable fuel electrodes than the classical Ni-YSZ. Only few metal-free fuel electrodes have been successfully proven in solid oxide cells. In particular, Tao et al. [20] proposed a simple perovskite with composition $La_{0.75}Sr_{0.25}Cr_{0.5}Mn_{0.5}O_3$ (LSCM) that showed high stability and performance as fuel electrode [21, 22]. A reasonable catalytic activity of these materials as oxygen electrodes was also proved, resulting in a remarkable performance in symmetrical SOFCs and SOECs [23, 24].

The present paper studies ytterbium scandium stabilized zirconia (YbScSZ) electrolyte-supported SOEC cell with symmetrical LSCM electrodes operating under different H_2O:CO_2 fuel compositions. Pure steam electrolysis, pure CO_2 electrolysis and different intermediate compositions of steam and CO_2 are evaluated. The paper compares the I-V curves obtained for this set of different fuels and compares them with the ones obtained by addition of safe gas (6% H_2). Only few studies of co-electrolysis with low percentages of safe gas have been previously published [,9, 10, 16, 25] and, to the best of our knowledge, this is the first that totally removes the hydrogen from the inlet fuel. Finally, H_2:CO production ratios are presented under different operation conditions.

Faraday Discussions Accepted Manuscript

Experimental method

Material synthesis, cell fabrication and characterization

$La_{0.75}Sr_{0.25}Cr_{0.5}Mn_{0.5}O_{3-\delta}$ (LSCM) powder was prepared by solid state reaction method using as precursors La_2O_3 (99.999% puratronic alfa aesar) Cr_2O_3 (99,6% alfa aesar), $MnCO_3$ (99,9% alfa aesar) y $SrCO_3$ (puratronic 99,994%, alfa aesar), mixed and heat treated in a single step at 1200°C-10h in air. The electrolyte was a tape casted disc of scandium and ytterbium stabilized zircon defined as $(ZrO2)_{0.9}(Yb2O3)_{0.06}(Sc2O3)_{0.04}$ ($Yb_{0.6}Sc_{0.4}SZ$ or YbScSZ) with 19.7 mm in diameter and 165 µm in thickness sintered at 1490° during 3h. The symmetrical LSCM electrodes were sintered at 1200-3h after deposition by airbrushing of an ethanol based LSCM ink. Painted and cured gold current collectors were employed for avoiding cross effects in the electrochemical response.

X-ray diffraction (XRD) was performed using a Bruker D8 Advanced diffractometer, equipped with a primary 80 monochromator and a LynxEye detector. The scans were performed in high resolution mode from 20 to 80° 2Ω range, using copper Kα1 radiation. XRD was used to analyze the phase purity of the as-synthesized LSCM powder and to evaluate the reactivity of the LSCM under different concentrations of CO_2 after 75h of exposition at 750°C and 900°C. Electrodes and electrolyte interfaces and morphology were studied by employing a Zeiss Auriga scanning electron microscope (SEM).

I-V polarization curves, galvanostatic aging test and Electrochemical Impedance Spectroscopy (EIS) measurements were carried out to evaluate the cell performance inside a Probostat test station (NorECS) at temperatures of 850-900°C by using a galvanostat/potentiostat with EIS capabilities (Parstat 2273, PAR). Figure 1 shows the experimental set up for the delivery of steam and CO_2 to the cell at the working temperature. The system permits the change of the gas composition and water content of the mixture. Ultrapure water is evaporated by a controlled

Faraday Discussions Accepted Manuscript

evaporator and mixing liquid delivery system (Bronkhorst-CEM system) that regulates and monitors the steam flow by a liquid flow controller. 50% of argon has been used as a carrier gas on the test station and the total flow of fuel has been balanced to 140ml/min. Micro gas chromatography (Agilent 490-µGC) was used to evaluate the concentration of produced H_2 and CO gases and H_2/CO ratio by a MolSieve 5A with Ar and He as respective carriers.

Faraday Discussions Accepted Manuscript

Experimental results

Characterization of the elements of the cell

Figure 2 shows an Arrhenius plot of the YbScSZ electrolyte conductivity. The values presented correspond to the deconvolution of the impedance spectra of symmetrical Pt/YbScSZ/Pt cells (not presented here). A remarkable improvement of the YbScSZ conductivity with respect to the state-of-the-art Yttrium stabilized zirconia defined as $(ZrO_2)_{0.92}(Y_2O_3)_{0.08}$ (8YSZ) electrolyte is observed (conductivity of 8YSZ is presented in the same figure for comparison). It is important to notice that working with YbScSZ allows employing electrolyte supported cells (thickness> 150µm) at temperatures above 800 °C. Therefore, a low enough resistance contribution to the cell is expected for the 165 µm thick electrolyte employed in this work at 850 °C. The conductivity of the electrolyte is in agreement with previously reported values for similar compositions [26, 27].

Figure 3 shows the XRD of the as-synthesized LSCM powders together with the diffraction patterns of the powder after being thermally treated during 75 hours in dry and wet CO_2 at temperatures between 750°C and 900°C. According to the XRD patterns, the as-synthesized LSCM presents a single phase, which remains stable to the carbonation under dry and wet CO_2 atmospheres at operating temperatures. The stability of the LSCM under typical co-electrolysis conditions of atmosphere and temperature shows a structural suitability of LSCM for this particular application.

An optimization study for the attachment temperature was carried out. Area specific resistance (ASR) of the cells was measured through the corresponding EIS spectra deconvolution. The optimal temperature to attach the LSCM on the YbScSZ electrolyte was determined to be 1200°C, which leads to an ASR = 0.5 $\Omega.cm^2$ at 900°C.

Faraday Discussions Accepted Manuscript

Cell performance under different fuel compositions

Figure 4 shows the I-V curves for a single symmetrical cell tested at 850 °C employing five different fuels: pure steam, pure CO_2 and three intermediate compositions with different H_2O:CO_2 ratio. Low values of OCV approaching zero were measured independently on the fuel. This is due to the absence of significant gradient of oxygen partial pressure across the cell before starting the electrolysis reactions. A maximum value of current density (780 mA/cm^2) was achieved when operates as a pure steam electrolyzer at 1.7 V. The maximum current density was progressively reduced for higher concentrations of CO_2 (Inset Figure 4). For pure CO_2 electrolysis, the maximum current density achieved was 700mA/cm^2 at 1.7 V. This decrease in the performance indicates that the reduction reaction of the carbon dioxide becomes the limiting step of the co-electrolysis mechanism [28]. In all cases, initial high resistances were observed at low current densities due to required activation potential of the electrodes at very low voltages. Current densities above 100 mA/cm^2 were required for reaching lower polarization resistances.

As previously mentioned, the whole set of measurements was repeated by adding safe gas (6% H_2) to the original fuel composition (Figure 5). OCV values close to 0.8V were observed independently on the fuel composition. These values are below the theoretical OCVs calculated by assuming a Nernst cell with a gradient of chemical potential based on the inlet fuel composition (OCV=0.94V) at the operation temperature and 6% of H_2. OCV cannot be accurately predicted by the standard calculations in the presence of water and CO_2 due to the effect of the reverse water shift reaction taking place all along the test station (RWSR: $CO_2+H_2 \rightarrow H_2O+ CO$)[29]. The best performance of the cell was achieved under pure steam electrolysis conditions (96%H_2O-6%H_2), injecting a current density of 600 mA/cm^2 at 1.7 V. Similar to hydrogen-free tests, the maximum ohmic resistance of the I-V curves was observed for the pure CO_2. However, in

Faraday Discussions Accepted Manuscript

this case, there is not clear correlation between the evolution of the maximum power and the CO_2 concentration in the fuel (Inset Figure 5). This is probably due to the promotion of the RWSR, i.e. the CO_2 dissociation, by the addition of the hydrogen safe gas in the inlet.

Comparison of the I-V curves presented in Figures 4 and 5 allows quantifying the effect of the addition of the safe gas in the cell performance. Cells operated with hydrogen-free fuels show even better performances. The lower performance of the cell in the presence of hydrogen can be ascribed to the reduction of the LSCM [21] . Maximum values of injected current densities are higher than previously published symmetrical cells and similar to reported values for classical cell configurations in co-electrolysis mode [4,10,30,31,32]. This indicates that the use of YbScSZ electrolyte supported cells with symmetrical electrodes of LSCM results in remarkable performances and allows eliminating the use of safe gas. This makes the system simpler and intrinsically protected from gas supply interruptions or unexpected incidents during operation.

Products composition in co-electrolysis mode

The composition of gas produced by LSCM/YbScSZ/LSCM cell operating in co-electrolysis mode was analyzed by µ-GC and compared for different inlet fuel compositions at 900°C. Figures 6a to 6c show the gas flow produced per active area of the cell and (if applicable) the H_2:CO ratio at two applied current densities (150 mA/cm^2 and 300 mA/cm^2) for different fuel compositions. In all the cases, the total produced gas is below the values predicted by the faraday law (dashed lines in the plots). Since the thermodynamics do not predict other reactions than the RWSR and the electrolysis of H_2O and CO_2 at the operation temperature and initial fuel compositions, the total amount of gas produced should accomplish the predicted values. The observed disagreement can be associated to small gas or current leakages. Although is not usually considered, the application of high voltages through the electrolyte generates a

Faraday Discussions Accepted Manuscript

significant electronic current (even in wide electrolytic domain materials such as stabilized zirconia [33]). The phase stability and electronic transport of the employed YbScSZ electrolyte under high applied voltages is currently under study for perfectly matching expected and measured gas productions.

Figure 6a shows the H_2 and CO generation for an atmosphere with the composition 50%H_2O–50%CO_2. Production rates per active area of 0.67ml/min.cm^2 of H_2 and 0.32ml/min.cm^2 of CO were detected when applying 150 mA/cm^2. Flows are almost twice these values when the current density is doubled (300 mA/cm^2), reaching production rates for H_2 and CO of 1.13 ml/min.cm^2 and 0.54 ml/min.cm^2, respectively. In both cases, H_2:CO ratios between 2.1-2.3 are maintained. Ratios close to 2 are highly desired for the synthetic fuel production using syngas as a precursor [10]. However, although co-elecectrolysis at low temperatures reaches the 2:1 ratio under regular working conditions [6,16,34], the operation at high temperatures requires low H_2 concentration in the inlet fuel to maintain high H_2:CO values. This is due to the fact that, at high temperatures, the RWSR can play an important role when a large amount of H_2 is added or high current densities are applied.

The composition of the produced gas was drastically modified when H_2 was introduced as safe gas in the inlet fuel (see figure 7). For injected density currents of 150 mA/cm^2, the production rates of H_2 and CO are 0.29 ml/min.cm^2 and 0.83 ml/min.cm^2, respectively, achieving very low H_2:CO ratio (0.35). Similarly, when doubling the current density to 300 mA/cm^2, a small ratio of H_2:CO = 0.67 is observed (with production rates of 0.73 ml/min. cm^2 of H_2 and 1.08 ml/min. cm^2 of CO). This behavior can be explained by means of the reverse water shift reaction. The high amount of H_2 introduced as a safe gas, promotes the displacement of the RWSR to the production of CO. Higher production of CO makes the H_2:CO ratio decrease. RWSR is typically reported for Ni electrodes [6,8,10,13,17], but it is clearly evidenced in the present work through the remarkable observed changes in the gas production selectivity. The RWSR

Faraday Discussions Accepted Manuscript

effect becomes more evident at low current densities because the added H_2 represents a higher fraction of the total amount of H_2 produced by the steam electrolysis. The relative increase of CO in the produced gas composition is roughly in agreement with the thermodynamics equilibrium calculation at operation temperatures of 900°C and 6% enriched H_2 fuel. Unfortunately, a precise calculation of the expected values is difficult because the complex balances among parallel catalytic reactions occurring at operation conditions [34]. The role of the RWSR can be so important that even questions the existence of a real electrochemical co-electrolysis. Some authors suggest that a maximum of 10% of CO is produced by RWSR at 800°C [35] while others conclude that only at high limiting current densities the CO_2 contributes to the electrochemical performance and the main production of CO is due to the thermo-chemical path [36].

Figure 8 shows the gas production rates for pure CO_2 electrolysis. CO flows of 0.85 ml/min cm^2 and 2.19 ml/min cm^2 were measured at current densities of 150 mA/cm^2 and 300 mA/cm^2, respectively. CO production becomes remarkable due to the increasing interest of CO_2 recirculation and revalorization. CO_2 electrolysis or co-electrolysis are some of the main routes to minimize the emissions of the produced CO_2 obtaining a product such as CO with a high added value.

Degradation of the cell in co-electrolysis mode

Figure 9 show the voltage evolution with time for a LSCM/YbScSZ/LSCM cell measured at 850 °C under galvanostatic conditions (300 mA/cm^2) in a hydrogen-free atmosphere with composition 50% H_2O- 50% CO_2. The voltage evolution observed in the galvanostatic test is in agreement with the observed evolution of the I-V curves (figure 10) obtained at different times of cell operation. From the starting I-V curve, it is possible to conclude a similar behavior to previously showed cells with current densities of 650 mA/cm^2 at 1.6V. An accelerated degradation is clearly observed after few hours of operation. It has to be highlighted that the performance of the

Faraday Discussions Accepted Manuscript

cell at the starting point is in accordance with the reported performance in co-electrolysis [8,10,11].

Further analyses performed by EIS in the operation point (Figure 11) show that the ohmic resistance is the main contribution of the dramatic cell degradation that takes place. Although the degradation during the first hour can be mainly attributed to an increase on the polarization resistance of the electrodes, the rapid increase of the ohmic resistance observed in EIS is clearly linked to the final failure. The initial ohmic resistance of 0.26Ωcm^2 reaches values of 1.25 Ωcm^2 after 6.5h of test (prior to collapse).

Post-mortem cross-section SEM images of the cell clearly point the focus of degradation in the electrolyte-oxygen electrode interface (Figure 12). Figure 12a show the oxygen-electrode/electrolyte interface before testing, while the figure 12 b show the equivalent interface after 7h of operation. There is a clear delaminating of the oxygen electrode likely due to the increase of oxygen pressure on the interface as previously described by other authors for the co-electrolysis mode [11,37,38,] and widely discussed on pure steam electrolysis [41-44]. Electrolyzer cells under operation are forced to generate a given amount of gas proportional to the current density applied. When the cathode is not catalytically active enough to transform the O^{2-} ions on O_2, or there is a poor diffusion of generated O_2, an over-pressure of oxygen is created. This overpressure starts to mechanically damage the interface leading to small pores or generating micro-cracks. This mechanism reduces the contact area between electrode and electrolyte exponentially. Reduction of contacting area increases the current density on the remaining contacting paths between electrode and electrolyte, accelerating the degradation process. Eventually, the initial generated micro porosity ends as a macroscopic discontinuity between the electrode and the electrolyte. This mechanism is consistent with the evolution of the impedance spectra observed from the LSCM symmetrical cells since the initial polarization resistance increase could correspond to a decrease of the active oxygen

Faraday Discussions Accepted Manuscript

reduction points on the oxygen electrode [40,43] . The final sudden increase of the ohmic resistance can be ascribed to the located depleting of the oxygen electrode. Depleted interface shown on figure 12b is representative of the effect of the described mechanism but is not present along the entire interface and it is probably magnified by the dismantling of the cell from the measurement station.

A complementary study of the evolution of the composition of the produced gas with time confirms the values of H_2 and CO production and H_2:CO ratio presented in the previous section (Figure 13). Two effects can be observed with the operation time: (i) a decrease of the hydrogen-to-carbon monoxide and (ii) a decrease of the gas production rate. Both phenomena could be explained by the continuous increase of the operation voltage due to the degradation process. On one hand, high voltages can activate selective electrolysis of the involved species and parallel catalytic reactions that alter the composition of the resulting gas [30]. On the other hand, as previously mentioned, high voltages (>1.7V) can produce the partial reduction of the YbScSZ electrolyte resulting in significant leakages of the applied current [33] (electrons going through the electrolyte without promoting any reaction). In this sense, some evidences of the creation of a monoclinic phase have been found by XRD analysis (Supplementary Figure S1) of the YbScSZ electrolyte after operation at voltages higher than 1.9V. This phase transformation has been related in the past with the electrolyte reduction and an increase of the electronic conductivity [44].

The strong delaminating and poor durability observed in the galvanostatic tests presented here should encourage further investigation on (i) ways for improving the catalytic activity of the LSCM electrode by, for instance, infiltration of functional active layers or improved microstructures [10,45] and (ii) reversible operation as recently proposed by Graves et al. [38].

Conclusions

Faraday Discussions Accepted Manuscript

A good electrochemical performance of full-ceramic LSCM/YbScSZ/LSCM SOEC cells was demonstrated in co-electrolysis mode for different fuel compositions. It was shown that no safe gas is required when using symmetrical full ceramic SOEC cells. The addition of H_2 in the initial fuel composition produces undesirable effects on the final H_2:CO ratios and could reduce the overall performance of the cell. Current densities above 700 mA/cm^2 at 1.7 V and 850 °C were applied in symmetrical cells for co-electrolysis tests based on hydrogen-free fuels. Moreover, ratios of H_2:CO about 2 were obtained, which are required for the synthesis of standard hydrocarbon fuels or alcohols. The study suggest that H_2:CO ratio can be tuned by changing the operation temperature, initial fuel composition and operation voltages. Despite these good results, significant degradation issues have been observed under galvanostatic operation conditions caused by the delaminating of the oxygen-electrolyte interface. This could be associated to an increase of the internal oxygen pressure close to the surface of the oxygen electrode. The use of more stable and more catalytically active functional layers is proposed as a solution for minimizing the delaminating problem together with the easy-to-integrate in symmetrical cells reversible operation mode (SOFC/SOEC).

Faraday Discussions Accepted Manuscript

Figures

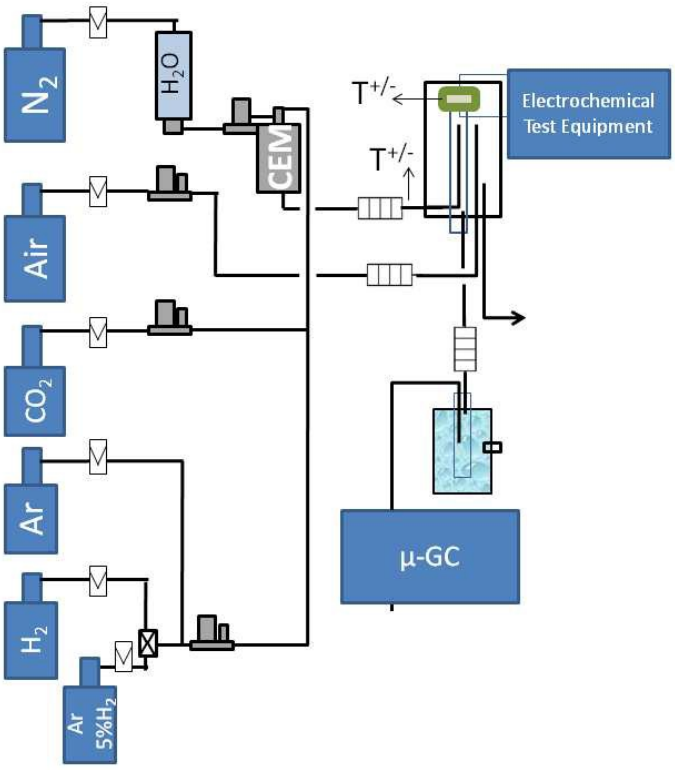

Fig. 1 Schematic diagram of the co-electrolysis test set up. The cell is placed to measure on the Probostat station where the temperature is controlled by different thermocouples in different places. The different gas flows are monitored by bronkhorst mass-flow controllers. Steam is produced and controlled by a Bronkhorst CEM and liquid flow controller system. Galvanostat/potentiostat Parstat 2273, PAR is used for the electrochemical measurements and Agilent μ-GC for the characterization of the produced fuel.

Faraday Discussions Accepted Manuscript

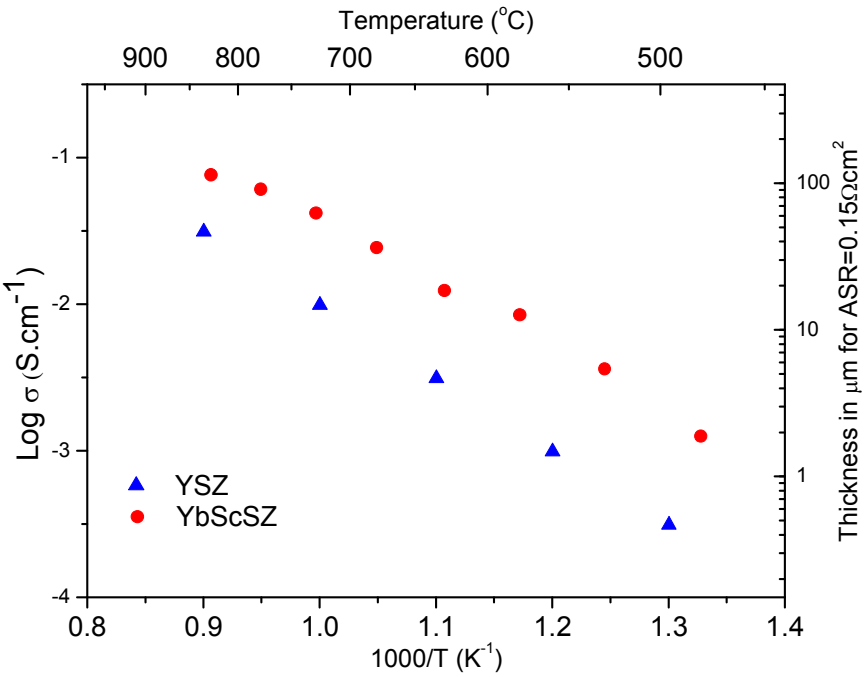

Fig 2 Arrhenius plot of the electrolyte conductivity as a function of the inverse of the temperature for YbScSZ and YSZ. The y-axis on the right shows the required thickness of the electrolyte for reaching an Area Specific Resistance ASR=0.15 Ωcm^2.

Faraday Discussions Accepted Manuscript

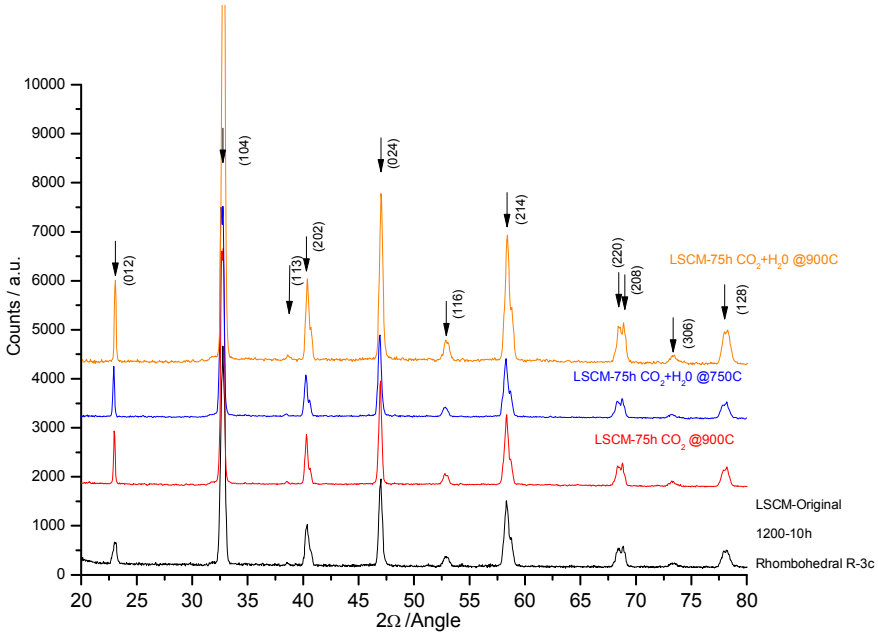

Fig 3. XRD of the as-synthetized LSCM and after heat treatments under different dry and wet CO_2 atmospheres. The original and treated LSCM show a rhomboedral crystallographic phase (SG *R-3c*) without noticeable secondary phases.

Faraday Discussions Accepted Manuscript

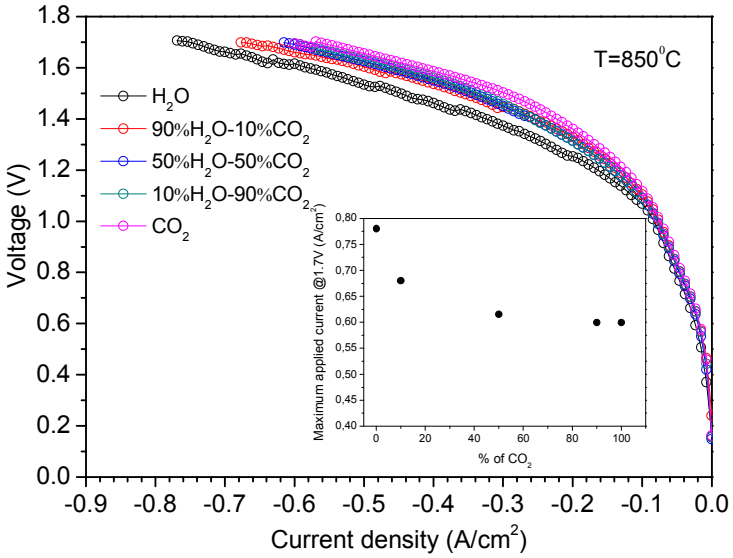

Fig 4. I-V curves of a symmetrical SOEC measured at 850ºC for different hydrogen-free fuel compositions. The insert shows the maximum current densityies obtained at 1.7V as a function of the CO_2 concentration.

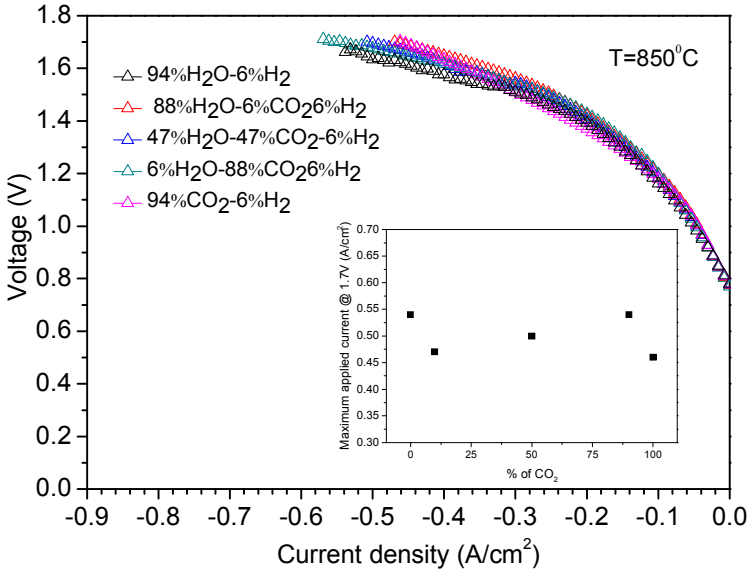

Fig 5. I-V curves of a symmetrical SOEC measured at 850ºC for different fuel compositions containing safe gas (6% H_2). The insert shows the maximum current densityies obtained at 1.7V as a function of the CO_2 concentration.

Faraday Discussions Accepted Manuscript

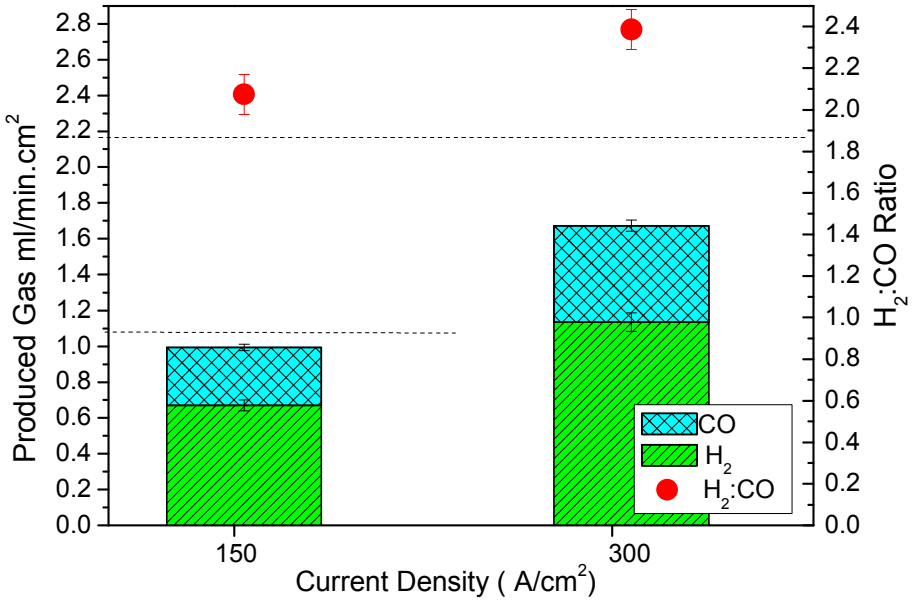

Fig.6 Gas flow per active area and composition (H_2:CO) of the products of a symmetrical SOEC operating at 900ºC under different applied current densities in a hydrogen-free atmosphere of 50%H_2O-50%CO_2. The red circles indicate the H_2:CO production ratio. The dashed lines indicate the theoretical total gas production according to the Faraday's law.

Faraday Discussions Accepted Manuscript

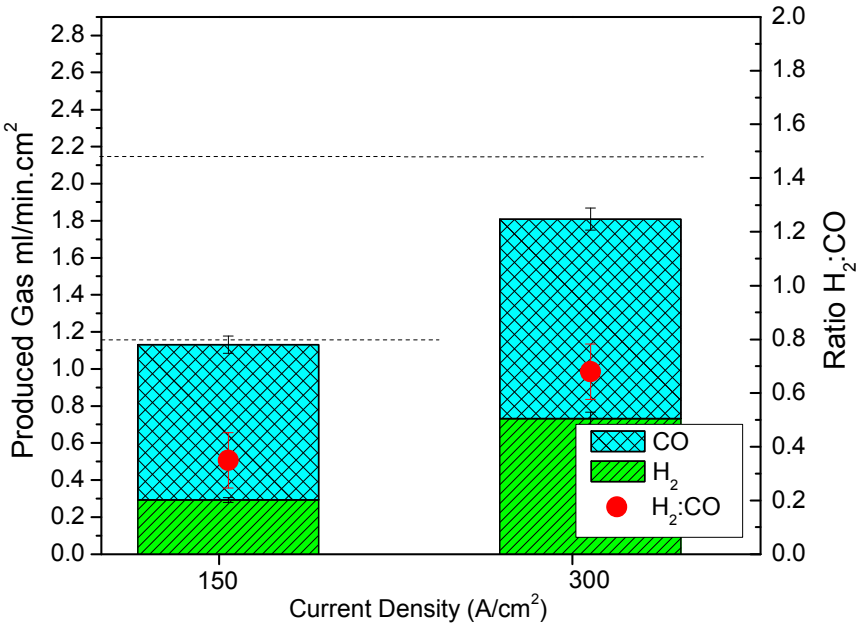

Fig.7 Gas flow per active area and composition (H_2:CO) of the products of a symmetrical SOEC operating at 900ºC under different applied current densities in an atmosphere of 47.5%H_2O-47.5%CO2 – 6%H_2 atmosphere. The red circles indicate the H_2:CO production ratio. The dashed lines indicate the theoretical total gas production according to the Faraday's law.

Faraday Discussions Accepted Manuscript

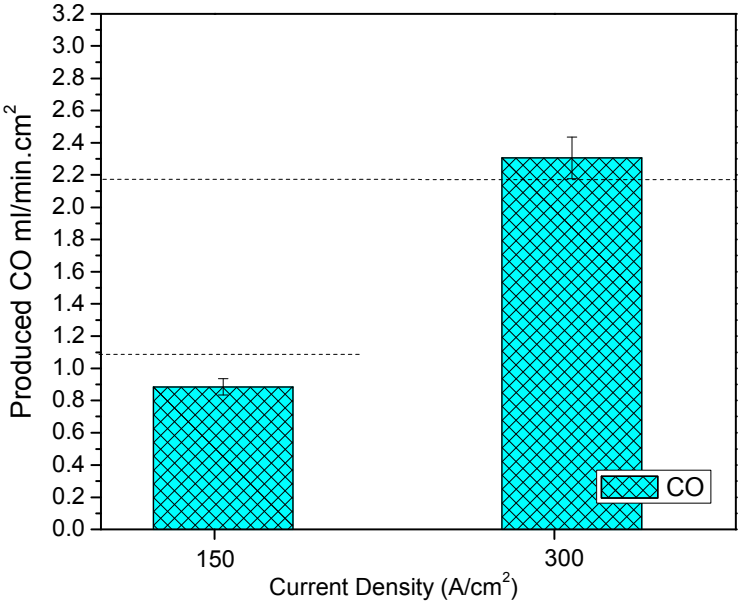

Fig.8 CO flow per active area of a symmetrical SOEC operating at 900ºC under different applied current densities in a pure CO_2 atmosphere. The dashed lines indicate the theoretical total gas production according to the Faraday's law.

Faraday Discussions Accepted Manuscript

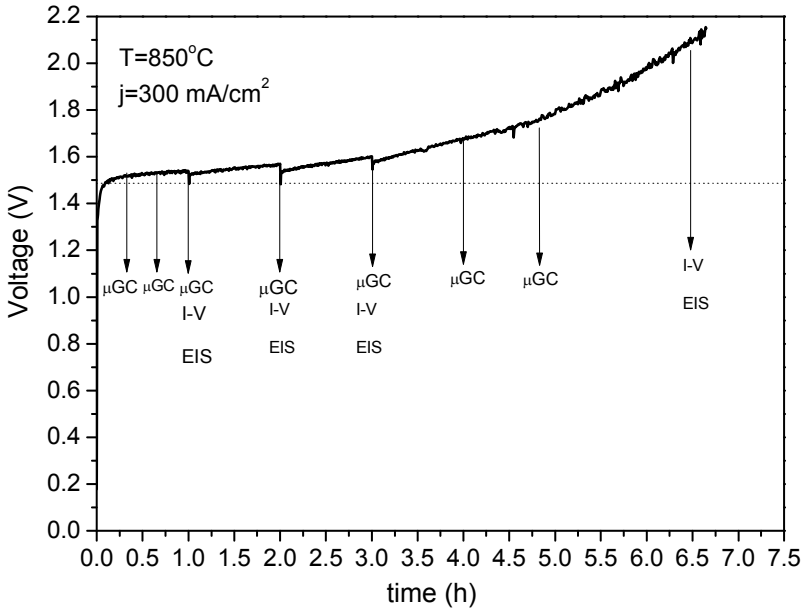

Fig. 9 Evolution of the voltage with time for a symmetrical cell operated under galvanostatic conditions (300 mA/cm^2) at 850ºC in 50%H_2O-50%CO_2 atmosphere. The arrows indicate the moment at which gas-chromatography analysis, I-V curves or EIS measurements were carried out. The solid line represents the thermoneutral potential for co-electrolysis.

Faraday Discussions Accepted Manuscript

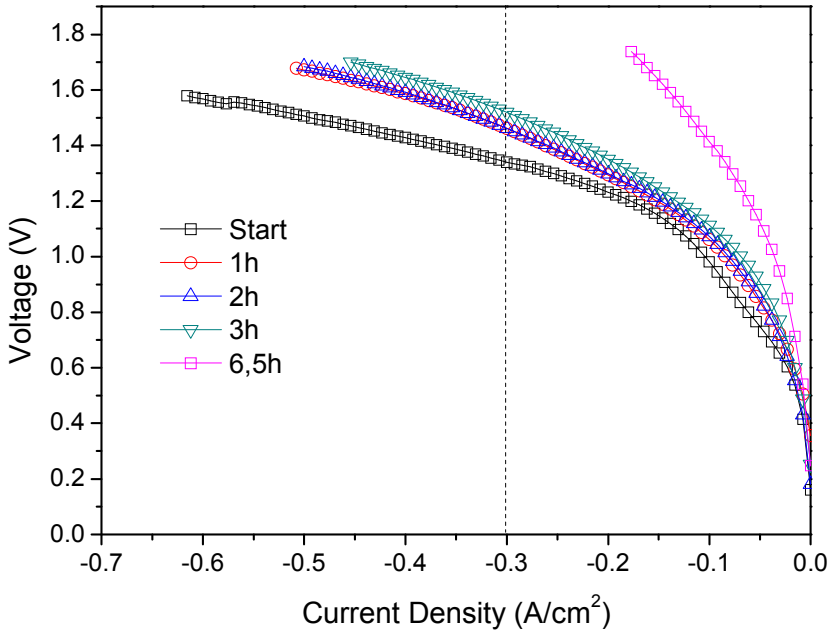

Fig. 10 I-V curves of the symmetrical cell at different times during the galvanostatic aging test (at a fixed current density of 300 mA/cm^2). The cell was operated at 850ºC and in 50%H_2O-50%CO_2 hydrogen-free atmosphere.

Faraday Discussions Accepted Manuscript

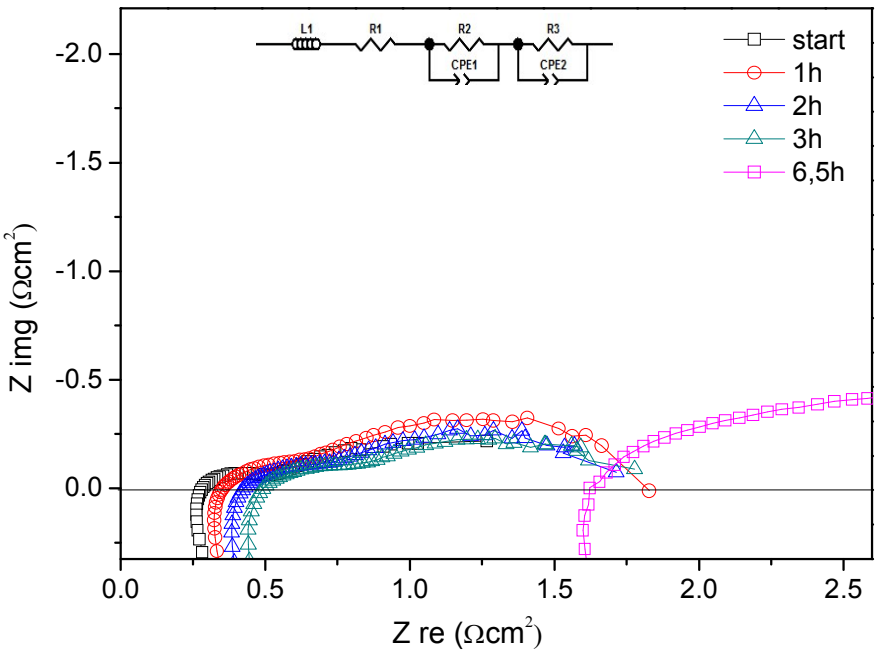

Fig. 11 Nyquist plot of the evolution with time of the impedance spectra obtained for the symmetrical cell during the galvanostatic test at a fixed current density of 300 mA/cm^2 at 850ºC in 50%H_2O-50%CO_2 hydrogen-free atmosphere.

Faraday Discussions Accepted Manuscript

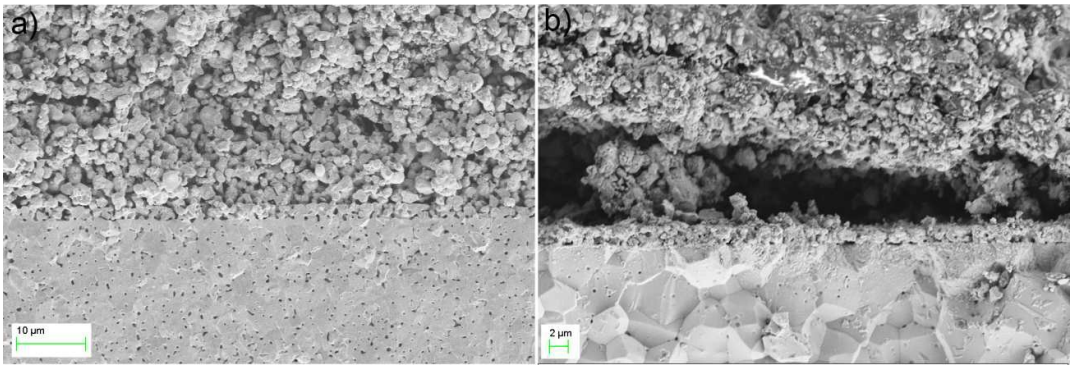

Fig 12 SEM cross sections of the LSCM/YbScSZ interlayer a) before and b) after 6.5h of galvanostatic test at a fixed density current of 300 mA/cm^2 at 850ºC in 50%H_2O-50%CO_2 hydrogen-free atmosphere.

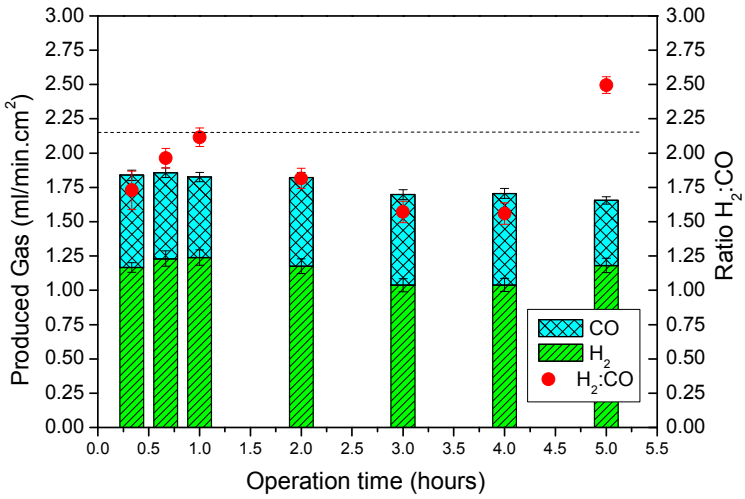

Fig.13 Evolution of the H_2 and CO production, and their relative ratio, during the first 5hours of the galvanostatic test at a fixed density current of 300 mA/cm^2 at 850ºC in 50%H_2O-50%CO_2 hydrogen-free atmosphere

Faraday Discussions Accepted Manuscript

References

[1] M. Aresta, A. Dibenedetto, A. Angelini, Chem. Rev. 114 (2014) 1709.

[2] A. Tarancón, C. Fábrega, A. Morata, M. Torrell, T. Andreu. Materials for Energy, Chapter: Power to fuel and artificial photosynthesis for chemical energy storage. Ed. D. Muñoz, X. Moya. Pan Stanford Publishing. 2015.

[3] C. Graves, S.D. Ebbesen, M. Mogensen, K.S. Lackner, Renew. Sustain. Energy Rev. 15 (2011) 1.

[4] X. Yue, J.T.S. Irvine, Solid State Ionics 225 (2012) 131.

[5] A. O. Isenberg, Solid State Ionics 3/4 (1981) 431.

[6] C. Stoots, J.E. O'Brien, J. S. Herring, J.J. Hartvigsen. J. Fuel Cell Sci. Technol. 6 (2008).

[7] Z. Zhan, W. Kobsiriphat, J.R. Wilson, M. Pillai, I. Kim, S.A. Barnett, Energy & Fuels 23 (2009) 3089.

[8] C. Stoots, Production of Synthesis Gas by H_2O and CO_2 (Coelectrolysis).Sustainable Fuels from CO_2, H_2O and Carbon free Energy Columbia University, New York, May 4, 2010.

[9] S. E. Yoon, S. H. Song, J. Choi, J.Y. Ahn, B.-K. Kim, J.S. Park, Int. J. Hydrogen Energy 39 (2014) 5497.

[10] C. Stoots, J. O'Brien, J. Hartvigsen, Int. J. Hydrogen Energy 34 (2009) 4208.

[11] P. Kim-Lohsoontorn, J. Bae, Proc. 2010 Eur. Solid Oxide Fuel Cell Forum 196 (2011) 7161.

[12] S. D. Ebbesen, C. Graves, M. Mogensen, Int. J. Green Energy 6 (2009) 646.

[13] H. Minfang, F. Hui, P. Suping, 12 (2014) 43.

[14] C.R. Graves "Recycling CO2 into Sustainable Hydrocarbon Fuels: Electrolysis of CO_2 and H_2O"; PhD by Columbia University, (2010).

[15] J. P. Stempien, O.L. Ding, Q. Sun, S.H. Chan, Int. J. Hydrogen Energy 37 (2012) 14518.

[16] Q. Fu, C. Mabilat, M. Zahid, A. Brisse, L. Gautier, Energy Environ. Sci. 3 (2010) 1382.

[17] C. Graves, S.D. Ebbesen, M. Mogensen, Proc. 17th Int. Conf. Solid State Ionics 192 (2011) 398.

[18] S. Uhm, Y.D. Kim, Curr. Appl. Phys. 14 (2014) 672.

[19] F. Bidrawn, G. Kim, G. Corre, J.T.S. Irvine, J.M. Vohs, R.J. Gorte, Electrochem. Solid-State Lett. 11 (2008) B167.

Faraday Discussions Accepted Manuscript

[20] S. Tao, J.T.S. Irvine, Nat. Mater. 2 (2003) 320.

[21] X. Yang, J.T.S. Irvine, J. Mater. Chem. 18 (2008) 2349.

[22] T. Delahaye, T. Jardiel, O. Joubert, R. Laucournet, G. Gauthier, M.T. Caldes, Solid State Ionics 184 (2011) 39.

[23] D.M. Bastidas, S. Tao, J.T.S. Irvine, J. Mater. Chem. 16 (2006) 1603.

[24] Q. Liu, X. Dong, G. Xiao, F. Zhao, F. Chen, Adv. Mater. 22 (2010) 5478.

[25] C. M. Stoots, J. E. O'Brien, K.G. Condie, J. J. Hartvigsen, Int. J. Hydrogen Energy 35 (2010) 4861.

[26] O. Yamamoto, Solid State Ionics 79 (1995) 137.

[27] V. Vijaya Lakshmi, Ranjit Bauri, Solid State Sci. 13 (2011) 1520

[28] W. Li, H. Wang, Y. Shi, N. Cai, Int. J. Hydrogen Energy 38 (2013) 11104.

[29] J.P. Stempien, Q. Liu, M. Ni, Q. Sun, S.H. Chan, Electrochim. Acta 147 (2014) 490.

[30] Y. Tao, S.D. Ebbesen, M.B. Mogensen J. of Electrochem. Soc. 161 (3) F337-F334 (2014)

[31] X. Yue, J.T.S. Irvine, J. Electrochem. Soc. 159 (2012) F442.

[32] S. D. Ebbesen, M. Mogensen, Sci. Adv. Fuel Cell Syst. 193 (2009) 349.

[33] T. H. Etsell, S.N. Flengas, J. Electrochem. Soc. 119 (1972) 1.

[34] W. L. Becker, R. J. Braun, M. Penev, M. Melaina, Asia-Pacific Forum Renew. Energy 2011 47 (2012) 99.

[35] J. Aicart, M. Petitjean, J. Laurencin, L. Tallobre, L. Dessemond, Int. J. Hydrogen Energy (2015).

[36] S. W. Kim, H. Kim, K.J. Yoon, J.H. Lee, B.K. Kim, W. Choi, J.-H. Lee, J. Hong, J. Power Sources 280 (2015) 630.

[37] A. V. Virkar, Int. J. Hydrogen Energy 35 (2010) 9527.

[38] C. Graves, S.D. Ebbesen, S.H. Jensen, S.B. Simonsen, M.B. Mogensen, Nat. Mater. (2014).

[39] R. Knibbe, M. L. Traulsen, A. Hauch, S. D. Ebbesen, M. Mogensen, J. Electrochem. Soc. 157 (2010) B1209.

[40] P. Hjalmarsson, X. Sun, Y.-L. Liu, M. Chen, J. Power Sources 223 (2013) 349.

[41] T. Jacobsen, M. Mogensen, in:, ECS Trans., ECS, 2008, pp. 259–273.

[42] F. Tietz, D. Sebold, A. Brisse, J. Schefold, J. Power Sources 223 (2013) 129.

Faraday Discussions Accepted Manuscript

[43] J. I. Gazzarri, O. Kesler, J. Power Sources 167 (2007) 100.

[44] A. Kumar, D. Rajdev, D.L. Douglas, J. Am. Ceram. Soc., 117, (1972) 378

[45] J. C. Ruiz-Morales, D. Marrero-López, J. Canales-Vázquez, J.T.S. Irvine, RSC Adv. 1 (2011) 1403.

Faraday Discussions Accepted Manuscript

Co-electrolysis of steam and CO_2 in full-ceramic symmetrical SOECs: A strategy for avoiding the use of Hydrogen as a safe gas.

M.Torrell[1], S. García-Rodríguez[2], A. Morata[1], G. Penelas[2], A. Tarancón[1]

[1] Catalonia Institute for Energy Research (IREC), Jardins de les Dones de Negre, 1, 08930-Sant Adrià de Besòs, Barcelona, Spain; *

atarancon@irec.cat

[2] REPSOL Technology Center, Ctra de Extremadura A-5, km 18, 28935 Móstoles, Madrid, Spain.

Suplementary information

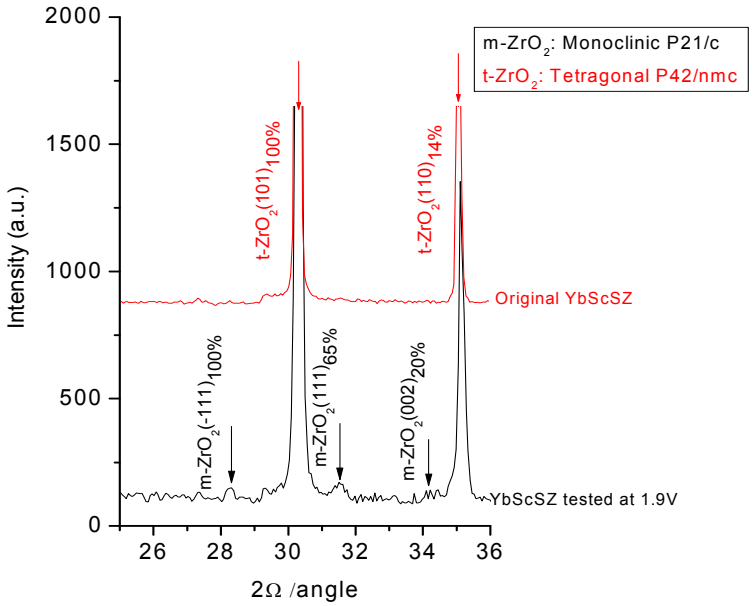

Figure S1. Detail of the XRD pattern of the original and tested YbScSZ at high voltage (1.9V) electrolyte where can be detected some evidences of monoclinic phase formation through the three main peaks of m-ZrO_2 not present in the original XRD pattern.

Faraday Discussions Accepted Manuscript